Article

JOURNAL OF ELASTOMERS & PLASTICS

Journal of Elastomers & Plastics
1–23

DOI: 10.1177/0095244318768634
journals.sagepub.com/home/jep
SAGE

Evaluation of the role of carbon nanotubes on the electrical properties of poly(butylene terephthalate) nanocomposites for industrial applications

A Dorigato[1], V Freitas[2], JA Covas[2], MC Paiva[2], M Brugnara[3] and A Pegoretti[1]

Abstract

In this article, innovative electrically conductive polymer nanocomposites based on poly(butylene terephthalate) (PBT) filled with carbon nanotubes (CNTs) at different concentrations, to be used in the automotive field, have been investigated. Field emission scanning electron microscopy (FESEM) analysis revealed how a good nanofiller dispersion was obtained, especially by using surface treated nanotubes and by processing these materials using a more restrictive screw configuration. Melt flow index measurements highlighted that the processability of these nanocomposites was reduced at elevated filler amounts, even if CNT surface treatment promoted a partial retention of the fluidity of the neat PBT. Thermal degradation stability was improved upon the addition of CNT, even at limited filler amounts. Differential scanning calorimetry measurements evidenced how the presence of CNT slightly increased both the crystallization temperature and the crystalline fraction of the materials. The additivation of CNTs promoted a stiffening effect at elevated CNT contents, associated to an evident embrittlement of the samples. Electrical resistivity measurements showed that the most interesting results (i.e. 2.6×10^{1} Ω·cm) were

[1] Department of Industrial Engineering and INSTM Research Unit, University of Trento, Trento, Italy
[2] Institute for Polymers and Composites/i3N, University of Minho, Guimarães, Portugal
[3] UFI Innovation Center Srl, Ala, Trentino, Italy

Corresponding authors:
A Dorigato, Department of Industrial Engineering and INSTM Research Unit, University of Trento, Via Sommarive 9, 38123 Trento, Italy.
Emails: andrea.dorigato@unitn.it

A Pegoretti, Department of Industrial Engineering and INSTM Research Unit, University of Trento, Via Sommarive 9, 38123 Trento, Italy.
Email: alessandro.pegoretti@unitn.it

obtained for nanocomposites with a total filler content of 3 wt%, processed using the more restrictive screw configuration. For these materials, it was possible to obtain a rapid surface heating through Joule effect at applied voltages of 12 V.

Keywords
Nanocomposites, carbon nanotubes, functionalization, conducting polymers, mechanical properties

Introduction

In the last decades, polymer matrix nanocomposites attracted considerable academic and industrial interest because the addition of inorganic nanostructured materials at limited concentrations can strongly improve the physical properties of polymer matrices, such as impact resistance,[1] elastic modulus,[2] dimensional stability, and thermal degradation resistance.[3–6] In general, polymeric materials are characterized by an elevated electrical resistance,[7] but in the last decades a wide variety of methods have been developed to reduce it.[8–14] One of the most interesting techniques is the additivation of conductive fillers such as carbon black (CB), CNTs,[15,16] graphene,[17–22] or metal particles. For instance, several nanocomposite systems were investigated by our group, considering different polymer matrices and conductive nanofillers.[23–27] It was widely demonstrated how above a critical filler concentration (i.e. percolation threshold) a conductive path within the polymer matrix, constituted by uninterrupted clusters of connected filler particles, can be constituted.[28–30] These materials could find wide application where charge dissipation and elevated electrical conductivity is required, for example, in the production of packaging films or sensitive electronic components, or materials subjected to corona treatments. One of the most critical technical issues is represented by the control of the filler dispersion quality, and an inhomogeneous dispersion in nanofilled systems could determine serious technical problems, such as heavy process dependency.[31–35]

Chemically speaking, poly(butylene terephthalate) (PBT) is a thermoplastic polyester obtained by polycondensation of 1,4-butanediol with either terephthalic acid or dimethyl terephthalate.[36] PBT was brought to market by Celanese in the late 1960s, and in 1970 fiber-reinforced PBT compounds were produced. Thanks to its easy processability and fast crystallization, PBT is a widely used thermoplastic polymer, and several injection moldable PBT grades are nowadays available on the market. Moreover, different mineral-filled, glass fiber–reinforced, impact-modified, and flame-retardant PBT grades, as well as several PBT-based blends are commercialized. PBT-based compounds are characterized by high strength and stiffness, low moisture absorption, excellent electrical properties and chemical resistance, and easy and fast moldability. PBT injection molded components are characterized by smooth surfaces that can be painted, printed, and ultrasonically welded. Because of its peculiar properties, PBT can be used in many products: appliances, automobiles, electrical and electronic parts, and industrial components. Because of its resistance to heat and

chemicals and the wide range of coloring possibilities, PBT is used for bobbins, connectors, switches, relays, terminal boards, motor brush holders, TV tuners, fuse cases, integrated circuit carriers, and sockets and end bells.

In addition to the production of injection molded parts, PBT can also be extruded as sheets, films, profiles, or as nonwoven fabrics. Nonwoven PBT polymer fabrics can be extensively used in air and liquid filters for the automotive field and industrial equipment.[37] Because of their high porosity, large surface area, dust free, low cost, easy processability and modifiability, these fabrics can also be applied for hygiene, family, and medical use. From a structural point of view, nonwovens are composed by a web of thin fibers, manufactured through different technologies (i.e. wet- or air-laid, spunbond, or melt-blown).

In the literature, only few works can be found on the effect of the addition of carbon nanotubes (CNTs) on the physical properties of PBT.[38–46] For instance, the influence of different carbon-based nanofillers (i.e. expanded graphite, CB, thermally reduced graphene oxide, and multi-walled CNTs (MWCNTs)) on the thermal, dielectric, electrical, and rheological properties of PBT was recently investigated by Yin et al.[46] It was demonstrated how carbon particles act as nucleation agents and significantly improved the main thermal properties of the material, and how CNT reaches the electrical percolation threshold at very low concentration (i.e. <0.5 wt%).

In some studies, innovative technological processes were utilized to prepare PBT/CNT nanocomposites. As an example, in the study by Saligheh et al., composite nanofibers of PBT/MWCNTs were prepared by electrospinning technique in the form of a web of random fibers. The effect of MWCNTs on the morphology, crystallinity, and mechanical properties of the resulting materials was investigated. The diameter, the crystallization temperature, and the mechanical properties of the prepared fibers were significantly affected by the incorporation of MWCNTs.[43] In the recent study by Gnanasekaran et al., fused deposition modeling was applied to print PBT/CNT nanocomposite materials having multifunctional properties.[39]

In a previous study by Dorigato et al., electrically conductive polymeric nanocomposites based on PBT filled with commercial CB and CNTs at different relative ratios have been developed.[47] It was demonstrated how the most interesting results were obtained for nanocomposites with a total filler content of 6 wt% and a CNT/CB relative amount equal to 2:1. The synergistic effect obtained with the combination of both nanofillers allowed a rapid surface heating through Joule effect even at applied voltages of 2 V. Moreover, in the recent study by Paiva et al., a solvent-free, one-pot functionalization of MWCNTs based on the 1,3-dipolar cycloaddition (DCA) of azomethine ylides using *N*-benzyloxycarbonyl glycine and formaldehyde was presented.[48] It was demonstrated how this simple, solvent-free chemical procedure could yield CNTs with fine-tuned surface functionality. A detailed description of this CNT functionalization was neglected here for the sake of brevity.

On the basis of these considerations, the objective of the present article is the development and the thermoelectrical characterization of PBT-based nanocomposites prepared through melt compounding, filled with CNTs at different amounts. A peculiar aspect of this work is the systematic investigation of the role played both by the CNT

surface functionalization and by the processing parameters on the physical properties of the resulting composites, in view of their future application in nonwoven fabrics. In fact, this research was carried out in collaboration with UFI Innovation Center Srl, a leading producer of solutions for fluid filtration in the automotive field (cars, motorbikes, etc.).

Even if the processing route adopted in this work is considerably different from the spinning utilized in nonwoven filters, the systematic investigation of the thermomechanical and electrical properties of PBT-based nanocomposites represents a preliminary (and necessary) experimental activity. In fact, this processing route provides a rapid manner to test the potential of the investigated materials to reach high electrical conductivity values and to be heated through Joule effect. The performed activity is therefore propaedeutic to the development of melt-blown filters.

Experimental part

Materials

Polymer pellets of PBT Lanxess Pocan B 1100 (density of 1300 g cm^{-3} and melt volume-flow rate at 250°C and 2.16 kg of 80 cm^3/10 min), provided by UFI Innovation Center Srl (UFI Filters Spa, Nogarole Rocca (VR), Italy), were utilized. NC7000 MWCNTs, synthesized by a catalytic carbon vapor deposition process, acquired from Nanocyl S.A. (Belgium), were considered as nanofiller. According to the supplier datasheet, their average length and diameter were 1.5 μm and 9.5 nm, respectively (aspect ratio 158).

Samples preparation

The surface functionalization of CNTs was carried out using the 1,3-DCA reaction of an azomethine ylide. In this solvent-free process, under the reaction conditions selected (reaction temperature of 250°C for 5 h), the chemical groups bonded to the CNT surface are mainly pyrrolidine. This mildly reactive amine is expected to bond with the ester groups in the polymer, as well as its end groups, under melt mixing conditions.[49] A detailed description of this functionalization procedure can be found elsewhere.[48]

PBT composites were prepared by melt mixing using a prototype corotating intermeshing mini twin-screw extruder with a screw diameter of 13 mm and length to diameter ratio of 27. The circular die channel presented a diameter of 3 mm. The temperature profile of the four heating zones along the length from hopper to die was set to 190°C, 235°C, 235°C, and 230°C. Two screw profiles were tested, formed by a different number and length of kneading zones, separated by conveying elements (as represented in Figure 1), in order to study the effect of mixing intensity upon the dispersion of the nanofillers in the PBT matrix. The various compositions were premixed in powder form and then compounded using a feed rate of 80 g h^{-1} and screw rotation speed of 80 rpm. Under these conditions, the average shear rates generated are within the range of those typically generated by larger machines. The extruded composites were cooled and pelletized. Moreover, the screw barrel is equipped with sample collecting

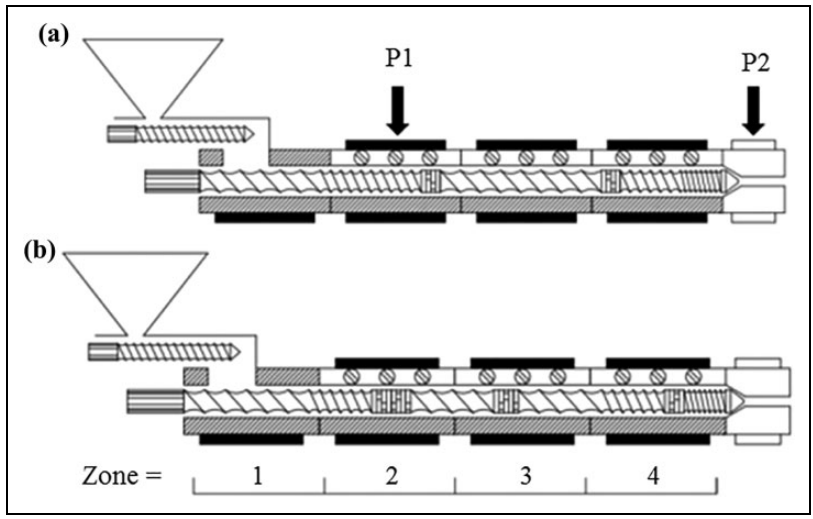

Figure 1. Schematic representation of the screw configurations used on the prototype corotating twin-screw extruder with indication of the sampling locations and heating zones.

Table 1. List of the prepared samples.

Sample	CNT content (wt%)	Screw configuration	Nanofiller
PBT	0	1	—
PBT-CNT-0.5	0.5	1	CNT
PBT-CNT-1.5	1.5		CNT
PBT-CNT-3	3		CNT
PBT-CNT-3F	3		Functionalized CNT
*PBT-CNT-3	3	2	CNT
*PBT-CNT-3F	3		Functionalized CNT

PBT: poly(butylene terephthalate); CNT: carbon nanotube.

devices along its length, allowing the collection of composite samples during steady-state extrusion operation conditions.[50] Samples were collected at locations P1 and P2 (Figure 1), the latter corresponding to the extrudate. The samples collected were immediately quenched in liquid nitrogen for subsequent characterization.

Compounded pellets were dried in a Moretto X Dry Air machine at 120°C for 24 h, and then compression molded at 250°C for 7 min under a pressure of 0.33 MPa, using a Carver Laboratory Press. In this way, square sheets (16 × 16 cm) with a thickness in the range from 1.0 mm to 1.2 mm were obtained. CNT-based nanocomposites with a filler content between 0.5 wt% and 3 wt% were prepared. In order to evaluate the effect of the surface functionalization and of the processing conditions on the physical properties of the resulting materials, nanocomposite samples with functionalized CNTs and/or processed with the screw configuration 2, with a

filler amount of 3 wt%, were produced. The list of the prepared samples is reported in Table 1.

Experimental methodologies

Scanning electron microscopy (SEM) of the as-received and functionalized CNT and of cryo-fractured composite surfaces sputtered with a combination of gold/palladium was performed on a NanoSEM FEI Nova 200 (FEI Company, Hilsboro, USA) . Optical microscopy of the composites cross sections was performed using a BH2 Olympus transmission optical microscope (Olympus Corporation, Tokyo, Japan) , for the analysis of the CNT dispersion in polylactic acid (PLA) . Thin composite sections with 5 μm thickness were cut directly from the extruded pellets using a Leitz 1401 microtome. At least five cuts were prepared for each composite, resulting in the observation of an average area of 6×10^5 μm^2 per sample. The images were acquired with a digital camera, LEICA DFC280 (Leica, Wetzlar, Germany) , coupled to the microscope. The Leica Qwin Pro software (Leica, Wetzlar, Germany) was used to measure the size and number of the CNT agglomerates, providing the agglomerate area distribution for each composite type, and the agglomerate area ratio, defined as the sum of all the agglomerate areas divided by the total composite area analyzed.

Melt flow index (MFI) measurements were carried out using a Dynisco melt indexer, model LMI 4000 Series (Dynisco LLC, Heilbronn, Germany) , according to ASTM D1238 standard, in order to evaluate the processability of the nanocomposites. For all the compositions, MFI was determined at a temperature of 250°C and under an applied weight of 5.0 kg.

Thermogravimetric analysis (TGA) was performed with a Mettler TG50 device (Mettler Toledo, Columbus, USA) in a temperature range of 30 to 700°C, at a heating rate of 10°C min^{-1}. Specimens were tested in air atmosphere at a flow rate of 100 mL min^{-1}. In this way, it was possible to evaluate the temperature associated to a mass loss of 5% ($T_{5\%}$), of 10% ($T_{10\%}$), the decomposition temperature T_d (corresponding to the temperature associated to the maximum mass loss rate) and the mass residue at 700°C (Wt_r). TGA under inert atmosphere was carried out on a modulated TGA Q500 from TA Instruments, heating the samples from room temperature to 700°C at 10°C min^{-1} under a constant nitrogen flow of 60 mL min^{-1}, and the weight loss was measured at 700°C to estimate the effective CNT content in each composite produced (Wt_{CNT}). Differential scanning calorimetry (DSC) measurements were carried out using a Mettler DSC30 calorimeter, performing three thermal ramps at 10°C·min^{-1}: a first heating from 0°C to 270°C, a cooling step from 270°C to 0°C, and a second heating from 0°C to 270°C. All the tests were carried out under a nitrogen flow of 100 mL min^{-1}. In this way, the glass transition temperature (T_g), the melting temperature (T_m), and the crystallization temperature (T_c) were determined. Moreover, the crystallinity content (X_c), obtained dividing the specific heat of fusion of the samples by the melting enthalpy of fully crystalline PBT, equal to 140 J g^{-1}, was determined.[51] The weight fraction of PBT in the composites was also taken into account.

Quasi-static tensile tests were performed with an Instron 4502 machine (Instron, Norwood, USA) , in order to determine the most important mechanical properties like elastic

modulus (E), stress at break (σ_b), and strain at break (ε_b). Tests for determination of the elastic modulus were performed using a load cell of 1 kN and a crosshead speed of 0.25 mm min^{-1}. An electrical extensometer with a gauge length of 12.5 mm was adopted. The experimental tests for determination of tensile properties at break were conducted using the same load cell but at a crosshead speed of 10 mm min^{-1}, without extensometer.

Electrical volume resistivity measurements of the PBT composites under direct current were carried out at room temperature with a Keithley 6517A electrometer (Keithley, Cleveland, USA) . Tests were performed at applied voltages of 2, 5, 10, 12, 20, 24, and 30 V, following the ASTM D-4496-04 standard. A four contact point configuration was adopted, with a distance of 3 mm between the measuring electrodes. Rectangular specimens (15 × 5 mm), with a thickness of about 0.6 mm, were tested. The resistivity (ρ) of the samples was determined through the following equation

$$\rho = R \cdot \frac{A}{L} \tag{1}$$

where R is the electrical resistance, A is the is the cross-sectional area of the specimens, and L is the distance between the measuring electrodes. The evolution of the surface temperature upon voltage applications was measured using a Fluke TiRx thermographic camera (Fluke, Everett, USA) , with the testing samples having a length of 35 mm and a width of 5 mm. The surface temperature was recorded after 5, 10, 30, 60, and 120 s starting from room temperature ($T_0 = 25°C$), under applied voltages of 12 and 24 V (i.e. the voltage levels available in the batteries of cars and trucks).

Results and discussion

It has been widely demonstrated that the macroscopic properties of nanofilled polymer composites are noticeably affected by the dispersion level of the nanofiller within the matrix. Therefore, the CNT agglomerates dispersion and morphology within PBT was analyzed at the micron scale using optical microscopy, and the dispersion and interface of individual CNT was analyzed by SEM.

The micrographs of the composites collected at positions P1 and P2, presented in Figure 2, illustrate the mixing effect along the screw length. A large number of CNT agglomerates is observed at P1, which is significantly reduced in P2 (composite at the die exit), demonstrating the efficiency of the dispersion process. The statistical analysis of the CNT agglomerate areas (A_{agg}) observed by optical microscopy provided relevant information for the characterization of the CNT dispersion state. In effect, the smaller the A_{agg} and the lower the number of agglomerates per unit composite area, the higher the dispersion state reached, meaning that a larger fraction of the CNT added was individually dispersed in the polymer. The agglomerate area ratio, A_R, measured as the ratio of the sum of the areas of all the agglomerates divided by the total composite area analyzed, may be used as an indicator of the dispersion level achieved. In fact, the larger the A_R the coarser the CNT dispersion is, meaning that a larger fraction of the CNT remains in agglomerated form. The analysis of the results presented in Table 2 shows that all the samples collected at P1 presented a coarser morphology, with larger A_R compared to the corresponding composites collected at the

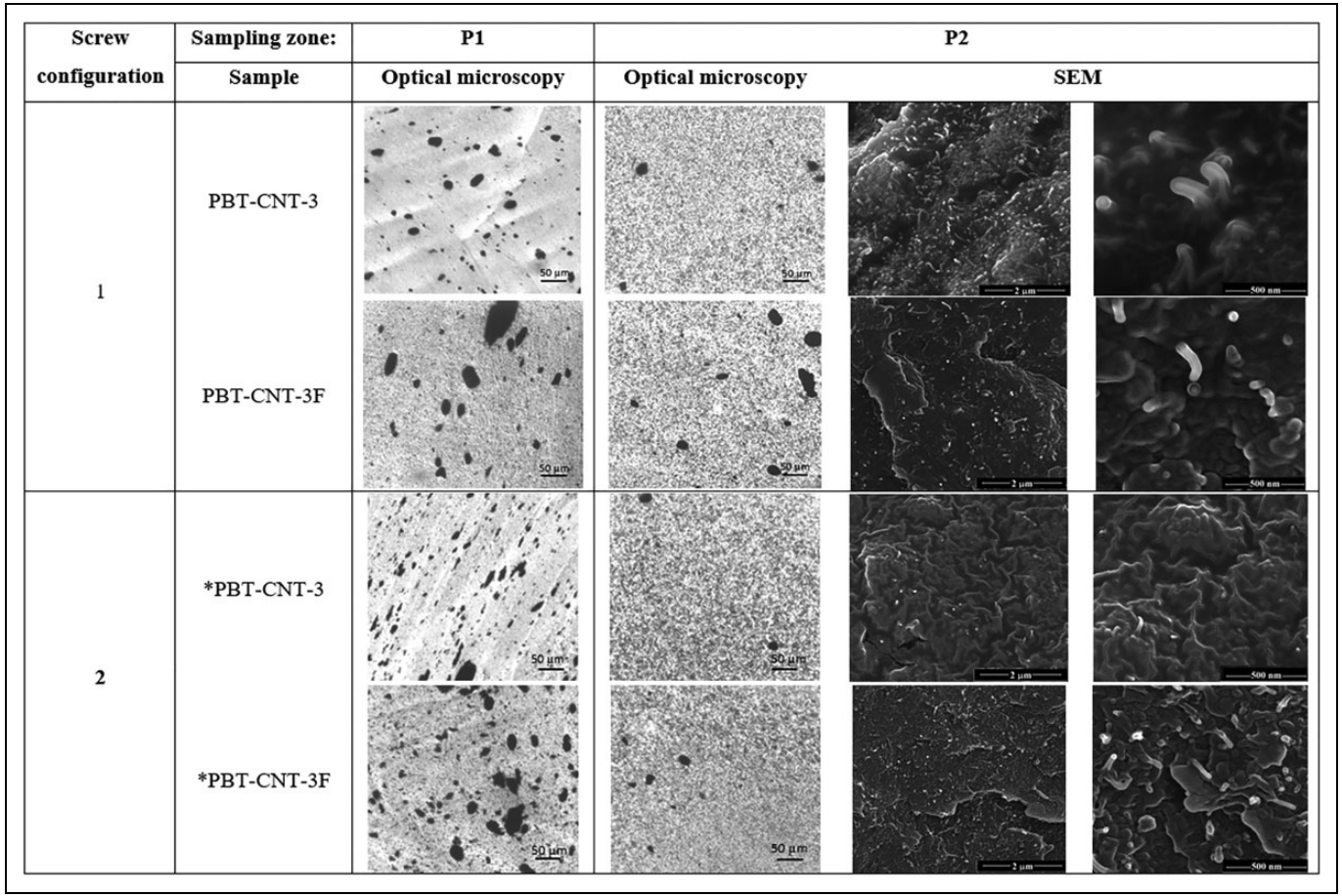

Figure 2. Optical microscopy and SEM characterization of the composites produced using two screw configurations. The samples collected at the first collection point (P1) were observed by optical microscopy only. SEM: scanning electron microscopy.

Table 2. Characterization of the non-dispersed CNT fraction in PBT composites with 3 wt% of as-received or functionalized CNT, collected at two different positions along the extruder screw, for composites produced using two different screw configurations.

Collection point	Screw configuration	Sample	Average agglomerate area (μm^2)	Area ratio	Number of agglomerates/mm^2
P1	1	PBT-CNT-3	83.1 ± 0.2	4.4	1179
		PBT-CNT-3F	106.0 ± 0.7	6.5	1267
	2	*PBT-CNT-3	66.6 ± 0.2	6.2	2052
		*PBT-CNT-3F	95.0 ± 0.2	9.3	2156
P2	1	PBT-CNT-3	69.2 ± 0.4	3.4	1091
		PBT-CNT-3F	80.0 ± 0.6	3.7	909
	2	*PBT-CNT-3	38.1 ± 0.4	1.2	681
		*PBT-CNT-3F	70.4 ± 0.8	2.0	610

PBT: poly(butylene terephthalate); CNT: carbon nanotube.

extruder die exit. Analysis of the data obtained for the composites collected at P2 shows that screw configuration 2 leads to better CNT dispersion, and thus to lower A_R, as well as lower agglomerate area and number. This is consistent with the optical micrographs shown in Figure 2. SEM images depict the CNT dispersed phase, showing a large amount of individually dispersed CNT across the composite cross section, and a general good CNT wetting by the PBT melt irrespective of the CNT surface treatment.

Considering the future application of the investigated materials and the hypothesized manufacturing process (melt blowing), it is important to evaluate their processability. In fact, it is well known how the viscosity of polymer matrices may strongly increase upon the addition of nanofiller, especially at elevated filler loading.[47] The measurement of the MFI provides an indicator of the composite processability, and thus of the possibility to produce electrically conductive filters that could be heated through Joule effect. The MFI test results are reported in Figure 3(a) and (b). As expected, as the nanofiller content in the composite increases, the MFI decreases (see Figure 3(a)). The drop in MFI is not dramatic up to a CNT content of 1.5 wt%, while it is strongly reduced for PBT-CNT-3 composite, decreasing nearly 60% compared to neat PBT. The incorporation of further nanofiller amounts is therefore technologically limited by the matrix viscosity. In fact, in order to preserve an acceptable processability level, a minimum MFI value of 20 g/10 min at a temperature of 250°C with an applied weight of 5.0 kg is indicated by the UFI Innovation Center Srl. Therefore, from the point of view of composite viscosity, it can be considered that all the prepared composites are potentially processable by melt blowing. In Figure 3(b), the MFI results of nanocomposite materials with 3 wt% of CNT are compared. It is evident that the composites prepared with functionalized CNTs show slightly higher MFI values compared to the corresponding composites with non-functionalized CNTs, irrespective of the adopted screw configuration. Functionalization of CNTs was observed to decrease the melt viscosity of the resulting composites[52] which may improve their processability. Also, a review by Cassagnau on the rheological

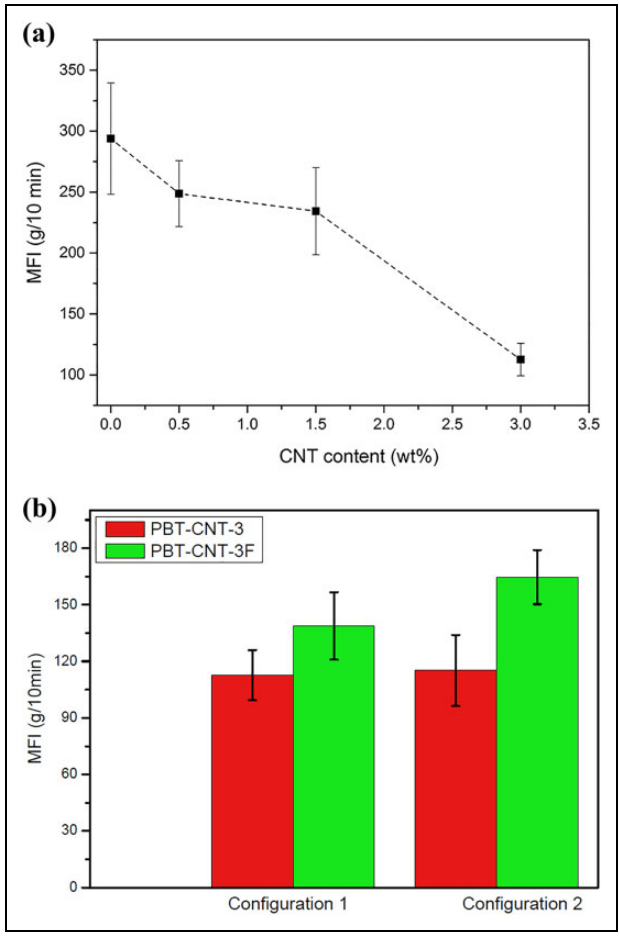

Figure 3. MFI values of neat PBT and relative nanocomposites: (a) effect of the CNT content and (b) effect of the CNT functionalization and of the screw configuration. MFI: melt flow index; PBT: poly(butylene terephthalate); CNT: carbon nanotube.

behavior of organoclay and fumed silica nanocomposites pointed out that the organic surface functionalization of the nanofillers leads to a decrease in the viscosity of the corresponding composites due to the breakdown in the particle interactions and the steric repulsion between functionalized nanofillers.[53] Conversely, the choice of the screw configuration did not strongly affect the viscosity of the prepared composites.

Considering the perspective application of these composites as melt-blown fibers for fabrics, the investigation of the influence of carbon-based nanofillers on the thermal properties of the resulting materials is important. Therefore, TGA tests were carried out on the prepared composites. In Figure 4, representative thermogravimetric curves of PBT nanocomposites with untreated CNTs at different concentrations are reported,

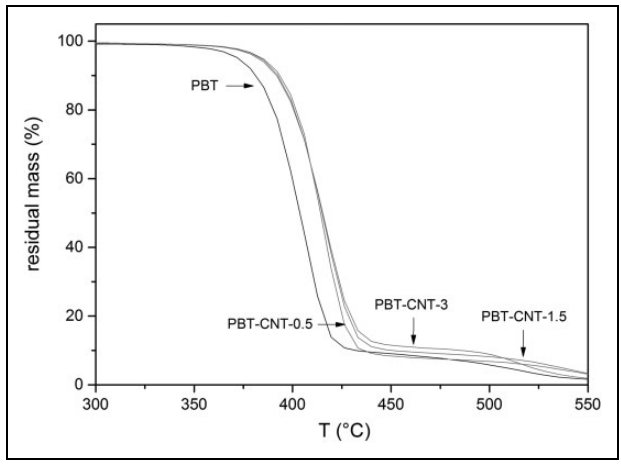

Figure 4. Thermogravimetric curves of neat PBT and relative nanocomposites (air atmosphere). PBT: poly(butylene terephthalate).

Table 3. Results of TGA analysis of neat PBT and nanocomposites (air atmosphere), and effective CNT content calculated from TGA results obtained under nitrogen atmosphere.

	Air atmosphere				N_2 atmosphere
Sample	$T_{5\%}$ (°C)	$T_{10\%}$ (°C)	T_d (°C)	Wt_r (%)	Wt_{CNT} (%)
PBT	372.3	381.1	399.7	0.4	—
PBT-CNT-0.5	384.6	393.3	410.5	0.2	0.4
PBT-CNT-1.5	383.6	392.4	410.6	0.0	1.4
PBT-CNT-3	382.3	391.7	410.6	0.1	2.9
PBT-CNT-3F	380.1	390.1	409.8	0.1	2.6
*PBT-CNT-3	375.2	385.5	404.5	0.3	3.2
*PBT-CNT-3F	372.6	383.5	404.8	0.2	2.9

TGA: Thermogravimetric analysis; PBT: poly(butylene terephthalate); CNT: carbon nanotube.

while in Table 3, the most important results are summarized. It is interesting to note how the addition of CNTs, even at low amounts, produces a noticeable increase in the thermal stability of the material, with an increase of $T_{5\%}$, $T_{10\%}$, and T_d parameters. For instance, with an addition of only 0.5 wt% of CNT, it is possible to increase the $T_{5\%}$ and the T_d values by about 12°C with respect to the neat PBT. According to the general theories on the flame resistance of polymer nanocomposites, the stabilization phenomena observed for these materials could be explained in terms of their ablative behavior.[54] In fact, during the thermal degradation of the specimen, CNTs may agglomerate on the surface of the molten polymer, thus creating a physical barrier that protects the rest of the polymer and hinders the volatilization of the oligomers generated during the combustion process. The ability to form this protective layer will depend on the capability of

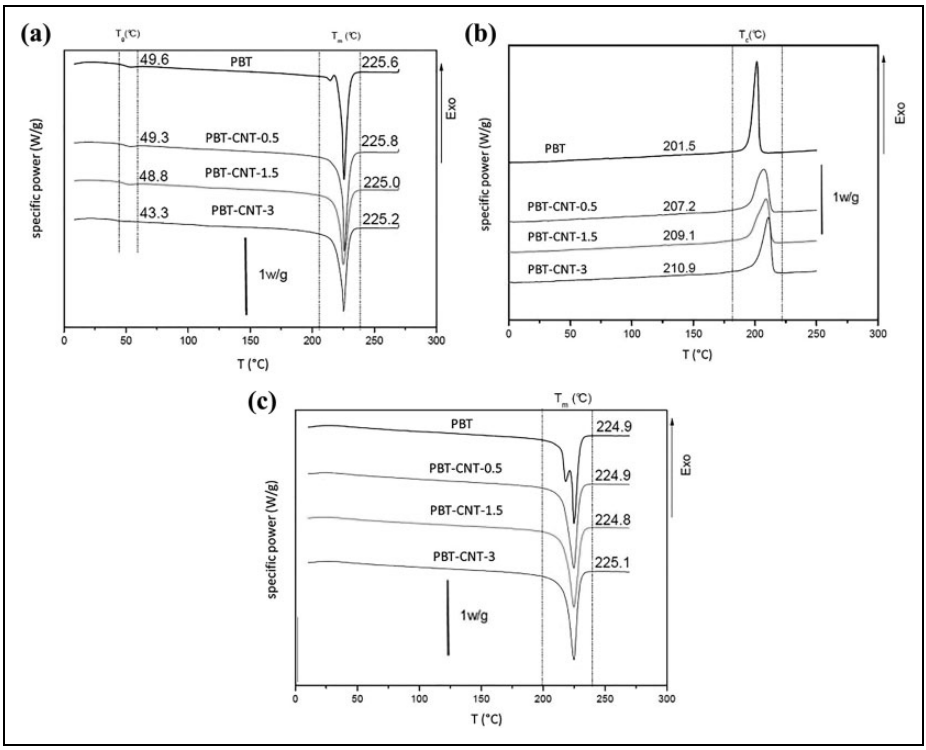

Figure 5. DSC thermograms of neat PBT and relative nanocomposites: (a) first heating stage, (b) cooling stage, and (c) second heating stage. DSC: differential scanning calorimetry; PBT: poly(butylene terephthalate).

nanofiller to form a continuous barrier. According to FESEM images reported in Figure 2, the fine individual dispersion of CNTs observed at all the considered concentrations allows the creation of an efficient barrier even at low filler amounts. It is also interesting to note how the functionalization of CNTs leads to a slight decrease in the thermal stability with respect to the composites with untreated CNTs at the same filler amount. As already reported by Garcia et al. and Leszczynska et al.,[55,56] this drop can be explained by the addition of less thermally stable organic moieties bonded to the CNT surface through functionalization. Furthermore, the change in the screw configuration determines a slight lowering in the thermal stability of the composite. It can be supposed that an increase in the thermomechanical stress to which the composite is subjected during the extrusion process leads to a slight thermal degradation of the compounds, with a consequent decrease in the molecular weight and thermal resistance. However, this hypothesis should be verified in the future with further analysis. As it could be expected, the residue left after TGA of all the samples in air is nearly zero, as both the organic components and the carbonaceous nanofiller decompose into gaseous products. TGA was also performed under inert atmosphere for the measurement of the real CNT content

Table 4. Results of DSC analysis of neat PBT and relative nanocomposites.

Sample	T_g (°C)	T_{m1} (°C)	X_c (%)	T_c (°C)	T_{m2} (°C)
PBT	49.6	225.6	40.9	201.5	224.9
PBT-CNT-0.5	49.3	225.8	43.5	207.2	224.9
PBT-CNT-1	48.8	225.0	43.6	209.1	224.8
PBT-CNT-3	43.3	225.2	43.7	210.9	225.1
PBT-CNT-3F	46.7	227.1	45.8	213.7	224.8
*PBT-CNT-3	44.5	225.4	44.4	210.7	224.9
*PBT-CNT-3F	44.0	224.7	43.8	210.2	224.8

DSC: differential scanning calorimetry; PBT: poly(butylene terephthalate); CNT: carbon nanotube; T_g: glass transition temperature (first heating stage); T_{m1}: melting temperature (first heating stage); X_c: crystallinity degree (first heating stage); T_c: crystallization temperature (cooling stage); T_{m2}: melting temperature (second heating stage).

Table 5. Results of quasi-static tensile tests on neat PBT and relative nanocomposites.

Sample	E (GPa)	σ_b (MPa)	ϵ_b (%)
PBT	2.38 ± 0.08	40.1 ± 5.4	1.5 ± 0.2
PBT-CNT-0.5	2.29 ± 0.07	31.9 ± 5.3	1.2 ± 0.2
PBT-CNT-1	2.21 ± 0.15	22.7 ± 4.3	0.8 ± 0.1
PBT-CNT-3	2.58 ± 0.10	18.7 ± 3.2	0.6 ± 0.1
PBT-CNT-3F	3.03 ± 0.05	26.6 ± 3.2	0.9 ± 0.1
*PBT-CNT-3	2.04 ± 0.32	13.9 ± 3.9	0.5 ± 0.1
*PBT-CNT-3F	2.46 ± 0.08	13.5 ± 5.1	0.5 ± 0.1

PBT: poly(butylene terephthalate); CNT: carbon nanotube.

of each composite. The CNT content was calculated accounting for the weight losses of neat PBT, neat CNT, functionalized CNT and their composites at 600°C, and the results are listed in Table 2. It could be noticed that the real CNT concentration in the prepared samples is near the theoretical one.

DSC tests were carried out in order to evaluate the effect of the addition of CNT on the thermal properties of the resulting composites. In Figure 5(a) to (c), representative DSC thermograms of nanocomposites with different CNT concentrations are reported, while the most important results are summarized in Table 4. It is clear that the melting temperature (T_m) of the material is not affected by the presence of nanofillers nor during the first neither in the second scan. Also the glass transition temperature (T_g) is not substantially influenced by the addition of nanofiller, and only a slight decrease in T_g (about 4°C) can be detected for a CNT loading of 3 wt%. As already reported in our previous study on PBT/CNT nanocomposites, the addition of CNT increases the crystallinity degree (from 41% of the neat PBT to 44% of the PBT-CNT-3 sample), irrespective of the presence of the surface functionalization and of the screw configuration. It could be therefore hypothesized that CNT acts as a nucleating agent on the polymeric matrix.[57] It is important to remind that

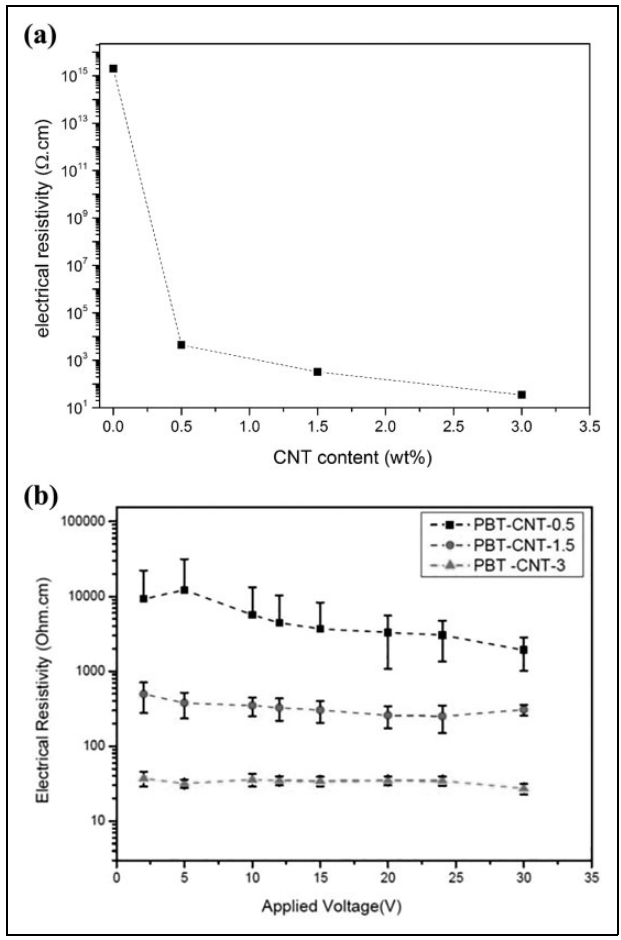

Figure 6. (a) Electrical bulk resistivity of PBT/CNT nanocomposites (applied voltage of 12 V) and (b) dependency of the electrical resistivity of PBT/CNT nanocomposites from the applied voltage. PBT: poly(butylene terephthalate); CNT: carbon nanotube.

one of the key parameters for the processing conditions of these materials is the crystallization temperature (T_c), because it determines the die-to-collector distance in the melt-blown technology. The results reported in Table 4 highlight that CNTs act as nucleating agents, with an increase of T_c with the CNT loading (up to 10°C with a CNT loading of 3 wt%). Even in this case, T_c values do not seem to be strongly influenced by CNT functionalization and/or by the screw configuration in the extrusion process.

The evaluation of the mechanical behavior of the tested materials plays a key role in the definition of their technological properties and, for the present application, in view of their future use as filters in the automotive field. In Table 5, the results of quasi-static

Table 6. Electrical resistivity values of PBT-based nanocomposites with a nanofiller content of 3 wt% (applied voltage 12 V).

Sample	Resistivity (Ω·cm)
PBT-CNT-3	3.5×10^{1}
PBT-CNT-3F	5.4×10^{3}
*PBT-CNT-3	2.6×10^{1}
*PBT-CNT-3F	4.6×10^{2}

PBT: poly(butylene terephthalate); CNT: carbon nanotube.

tests performed on the prepared nanocomposites are summarized. Considering the standard deviation values associated to these measurements, it can be concluded that the stiffness of the composites is not substantially affected by the addition of nanofiller until a CNT content of 1.5 wt%, and only for the nanocomposite filled at 3 wt% a slight increase of the elastic modulus (less than 10%) can be detected. The surface functionalization tends to further improve the stiffness of the material, probably because of the improved CNT/PBT interface, while a change in screw configuration in the extrusion process tends to decrease the elastic modulus. Comparing these results with those from MFI tests (see Figure 3(b)), it could be hypothesized that the harsher conditions applied to the composite melt under screw configuration 2 could promote its partial thermal degradation, with a consequent reduction in the elastic and rheological properties of the resulting materials. As it often happens with nanofilled systems, an increase in the nanofiller concentration leads to an evident embrittlement of the samples, with a consequent decrease of the stress at break (σ_b) and of the strain at break values (ε_b). The presence of the surface functionalization, with the improvement of the CNT/PBT interface, seems to promote a partial retention of the failure properties of the pristine polymer (at least in screw configuration 1), while a change in screw configuration probably promotes the thermal degradation of the matrix, with a reduction of the σ_b and ε_b values.

Four point probe electrical measurements were carried out, and the results of volume resistivity measurements on the samples containing untreated CNTs at an applied voltage of 12 V are reported in Figure 6(a). The introduction of the carbon-based nanofiller in the insulating polymeric matrix increases the conductivity of the nanocomposites. As an example, a resistivity value lower than 10^2 Ω·cm can be achieved with a CNT content of 3%wt. The percolation threshold for the prepared composites is very low (less than 0.5 wt%). In the previous study of Dorigato et al. on PBT nanocomposites,[47] a resistivity of 10^3 Ω·cm was reached with a CNT content of 6 wt%. It may be therefore concluded that the twin-screw melt mixing technique led to a better nanofiller dispersion within the matrix, with a consequent increase in conductivity. Based on the information obtained by UFI Innovation Center Srl, a target volume resistivity value lower than 10^3 Ω·cm at an applied voltage of 12 V is required to prepare nanocomposites that could be effectively heated through Joule

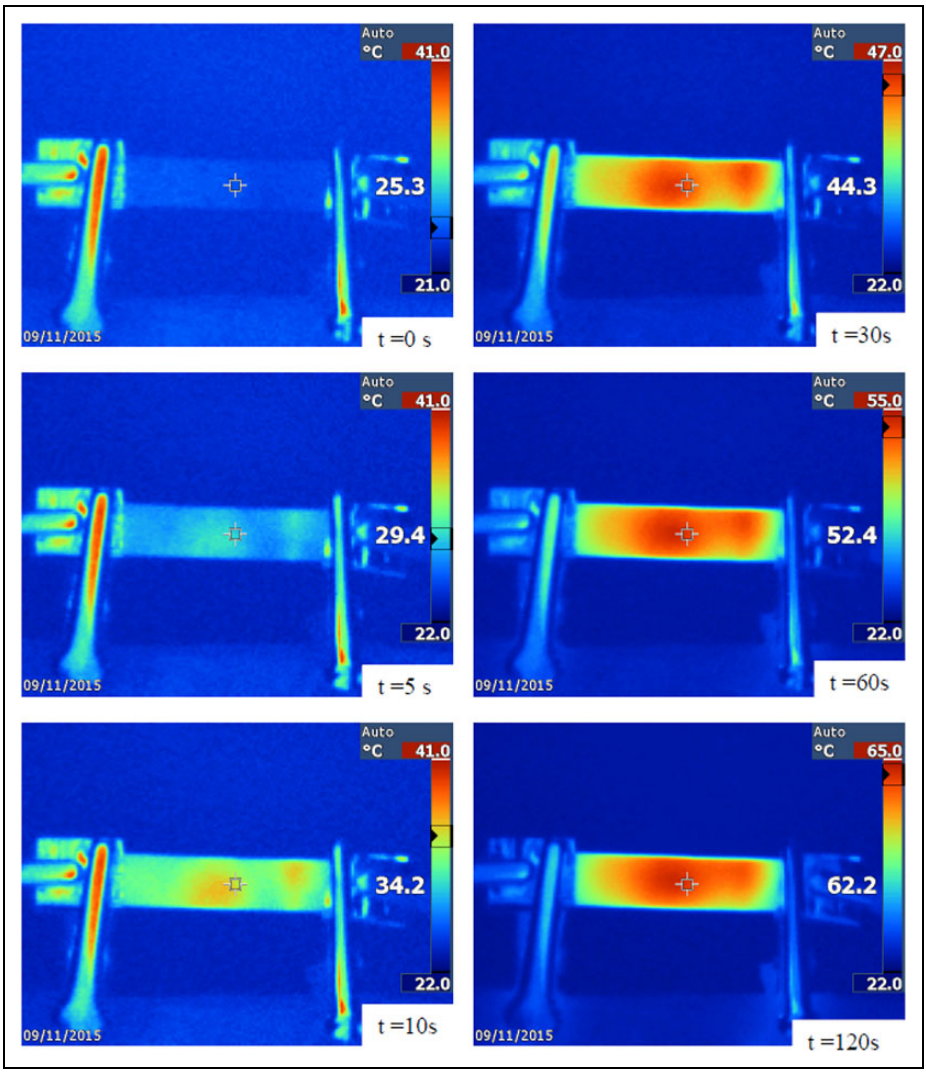

Figure 7. Thermocamera images of surface temperature evolution upon voltage application of *PBT-CNT-3 sample at an applied voltage of 24 V. PBT: poly(butylene terephthalate); CNT: carbon nanotube.

effect. For this reason, CNT-filled nanocomposites with a filler amount higher than 1.5 wt% could be potentially applied for the required application. Moreover, from Figure 6(b), it can be concluded that the nanofilled samples with CNT content higher than 1.5 wt% present an Ohmic behavior, being the electrical resistivity values independent from the applied voltage. It is also important to evaluate the effect of

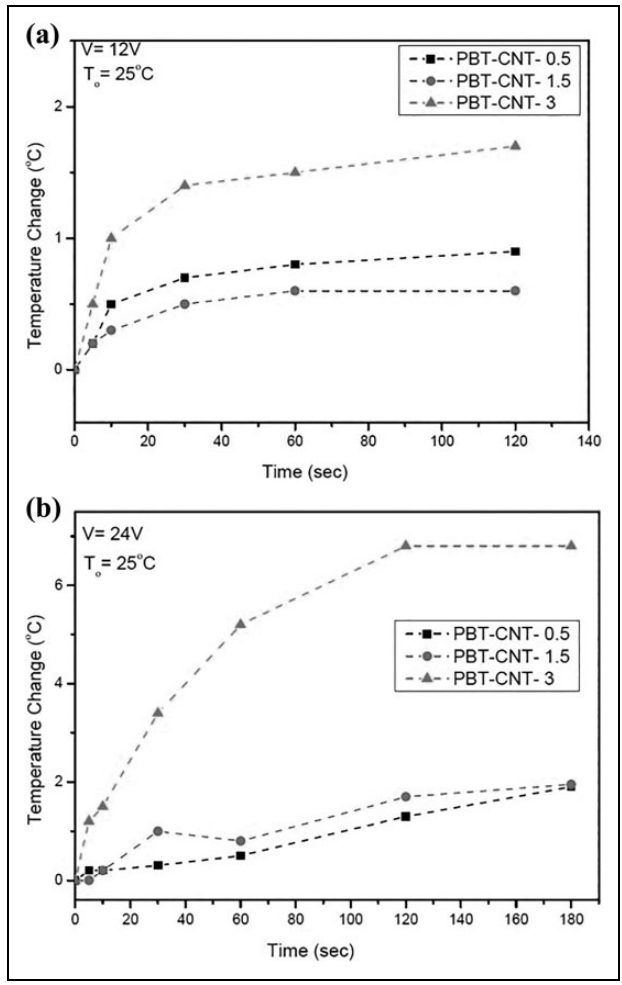

Figure 8. Surface temperature evolution of PBT-based nanocomposites at an applied voltage of (a) 12 V and (b) 24 V. PBT: poly(butylene terephthalate) .

CNT functionalization and of the screw configuration on the electrical properties of the prepared materials.

In Table 6, electrical resistivity values of PBT-based nanocomposites with a nano-filler content of 3 wt%, tested at a voltage of 12 V, are summarized. It is interesting to note how the presence of the surface functionalization determines a substantial decrease in the electrical conductivity of the samples. It is possible that the presence of the organic layer around CNTs hinders the electronic conduction within the materials, even if a percolative network is formed. This hypothesis is also supported by the study by Costa

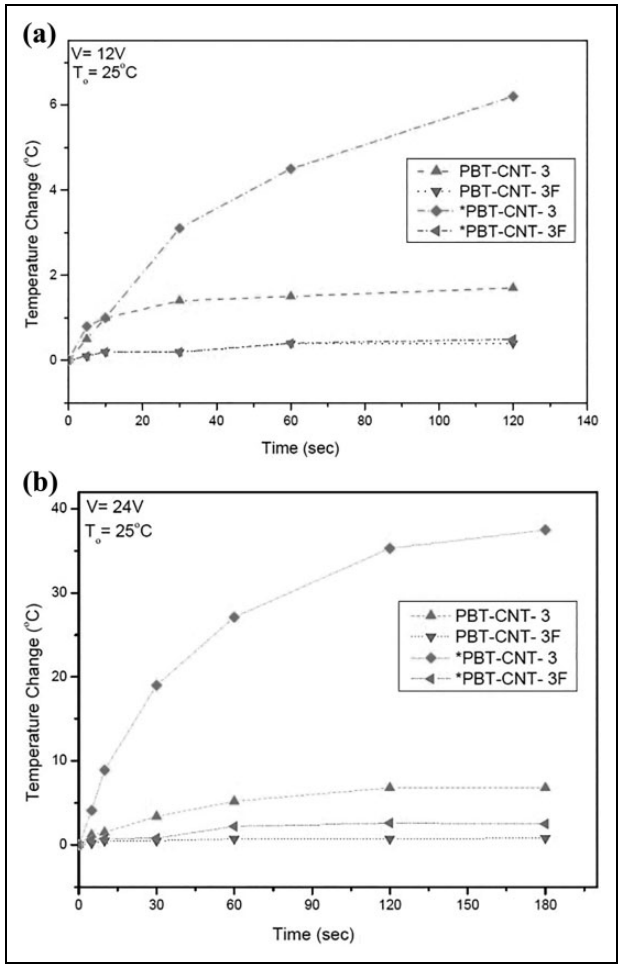

Figure 9. Surface temperature evolution of PBT nanocomposites with a CNT content of 3 wt% at an applied voltage of (a) 12 V and (b) 24 V. PBT: poly(butylene terephthalate); CNT: carbon nanotube.

et al., in which the effect of CNT type and functionalization on the electrical, thermal, mechanical, and electromechanical properties of CNT/styrene–butadiene–styrene composites was investigated.[58] Moreover, processing these materials under more intensive mixing conditions (i.e. screw configuration 2) leads to a slight improvement of the electrical conductivity, probably due to better nanofiller dispersion within the matrix (see FESEM micrographs in Figure 2).

The heating capability of PBT nanocomposites was evaluated through a thermo-camera. In Figure 7, representative images of the evolution of the surface temperature of *PBT-CNT-3 composite sample at an applied voltage of 24 V are reported. An effective

heating is evident even after 10 s, and a temperature of 62°C can be reached after 120 s. In Figure 8(a) and (b), the measurements of Joule heating of the samples containing untreated CNTs at 12 V and 24 V are, respectively, reported. The evolution of the surface temperature with respect to the applied voltage and to the composition of the nanocomposites was measured. It is interesting to see how at 12 V the heating capability of the tested materials is rather limited, and only with the PBT-CNT-3 composite is possible to reach a slight heating of the sample (i.e. less than 2°C after 120 V). The heating ability is improved by running the test at 24 V (see Figure 8(b)). However, even in this case only the PBT-CNT-3 shows a significant surface temperature increment after 120 s (about 7°C). The effect of the nanofiller surface treatment and of the processing conditions should also be analyzed. In Figure 9(a) and (b), surface temperature evolution of PBT nanocomposites with a CNT content of 3 wt% at applied voltages of 12 V and 24 V are, respectively, reported. From these plots, it can be concluded that the presence of the surface functionalization, hindering the electrical conductivity properties of the samples, does not allow the heating of the samples, regardless of the applied voltage. Conversely, processing with screw configuration 2, with the consequent improvement of the nanofiller dispersion and thus of the electrical conductivity, leads to the achievement of an interesting increase in the surface temperature of the materials, especially at elevated voltage. For instance, with the *PBT-CNT-3 composite, it is possible to reach a temperature increase of 37°C after 180 s at 24 V. It can be therefore concluded that the results of surface heating measurements are in agreement with the results reported for electrical resistivity tests (see Figure 6; Table 6). The samples that present the higher conductivity dissipate more thermal power, and in these conditions the surface heating is more intense. Finally, another interesting aspect observed for the samples with higher conductivity is that during the first seconds of heating, there is a rapid increase in temperature, and the material reaches a temperature plateau, due to the fact that the thermal power produced is equal to the dissipated one. This aspect is of key importance for the application of these materials as filters, because the thermal degradation of the materials for prolonged voltage application times should be avoided.

Conclusions

Novel electrically conductive nanocomposites based on PBT filled with CNTs at different amounts were investigated. FESEM micrographs demonstrated how a good nanofiller dispersion was achieved, especially by using surface treated nanotubes and by processing the composites by twin-screw extrusion. MFI measurements demonstrated how the processability of the nanocomposites was reduced at elevated filler amounts. Thermal degradation stability was improved upon the addition of CNT, even at low filler contents. The addition of CNT promoted an interesting nucleating capability of the PBT matrix, with an enhancement of the crystallization temperature and the crystallinity degree. The addition of CNTs determined a stiffening effect at elevated filler amounts, accompanied by an evident embrittlement of the samples.

The addition of nanofiller above the percolation threshold allowed to considerably improve the electrical conductivity of the samples. Electrical resistivity values of about

10 Ω·cm were obtained for nanocomposites with an untreated CNT amount of 3 wt%. With this composition, it was possible to obtain a rapid surface heating through Joule effect at applied voltages of 12 V.

Acknowledgements

The authors gratefully acknowledge Minlargilih Melak Amare for his collaboration in the experimental activities. The authors also acknowledge the Portuguese Foundation for Science and Technology (FCT) for project PEst-C/CTM/LA0025/2013 (LA 25—2015–2017).

Declaration of Conflicting Interests

The author(s) declared no potential conflicts of interest with respect to the research, authorship, and/or publication of this article.

Funding

The author(s) disclosed receipt of the following financial support for the research, authorship, and/or publication of this article: This research activity has been supported by Fondazione Cassa di Risparmio di Trento e Rovereto (CARITRO) within the project "Bando Caritro 2014 per progetti di ricerca scientifica finalizzati allo sviluppo di iniziative imprenditoriali." The work was also supported by the National Interuniversitary Consortium of Materials Science and Technology (INSTM).

ORCID iD

M Brugnara http://orcid.org/0000-0002-8722-8926

References

1. Rong M, Zhang M and Zheng Y. Improvement of tensile properties of nano-SiO2/PP composites in relation to percolation mechanism. *Polymer* 2001; 42: 3301–3304.
2. Agag T, Koga T and Takeichi T. Studies on thermal and mechanical properties of polyimide-clay nanocomposites. *Polymer* 2001; 42: 3399–3408.
3. Fu X and Qutubuddin S. Synthesis of polystyrene-clay nanocomposites. *Mater Lett* 2000; 42: 12–15.
4. Shelley JS, Mather PT and De Vries KL. Reinforcement and environmental degradation of nylon-6/clay nanocomposites. *Polymer* 2001; 42: 5849–5858.
5. Shu Z, Chen G and Qi Z. Polymer/clay nano-composite and its unique flame retardance. *Plast Ind* 2000; 28: 24–26.
6. Uhl FM and Wilkie CA. Polystyrene/graphite nanocomposites: effect on thermal stability. *Polym Degrad Stab* 2002; 76: 111–122.
7. Norman RH and Boonstra BB. Conductive rubbers and plastics. *J Polym Sci B Polym Lett* 1972; 10: 479.
8. Armand M. Polymers with ionic conductivity. *Adv Mater* 1990; 2: 278–286.
9. Ibidapo TA. Classification of ionic polymers. *Polym Eng Sci* 1988; 28: 1473–1476.
10. Masoud EM. Citrated porous gel copolymer electrolyte composite for lithium ion batteries application: an investigation of ionic conduction in an optimized crystalline and porous structure. *J Alloys Compound* 2015; 651: 157–163. DOI: 10.1016/j.jallcom.2015.08.079.

11. Masoud EM. Nano lithium aluminate filler incorporating gel lithium triflate polymer composite: preparation, characterization and application as an electrolyte in lithium ion batteries. *Polym Test* 2016; 56: 65–73. DOI: 10.1016/j.polymertesting.2016.09.024.
12. Masoud EM, El-Bellihi AA, Bayoumy WA, et al. Effect of LiAlO2 nanoparticle filler concentration on the electrical properties of PEO–LiClO4 composite. *Mater Res Bull* 2013; 48: 1148–1154. DOI: 10.1016/j.materresbull.2012.12.012.
13. Masoud EM, El-Bellihi AA, Bayoumy WA, et al. Organic–inorganic composite polymer electrolyte based on PEO–LiClO4 and nano-Al2O3 filler for lithium polymer batteries: dielectric and transport properties. *J Alloys Compound* 2013; 575: 223–228. DOI: 10.1016/j.jallcom.2013.04.054.
14. Masoud EM, Hassan ME, Wahdaan SE, et al. Gel P (VdF/HFP)/PVAc/lithium hexafluorophosphate composite electrolyte containing nano ZnO filler for lithium ion batteries application: effect of nano filler concentration on structure, thermal stability and transport properties. *Polym Test* 2016; 56: 277–286. DOI: 10.1016/j.polymertesting.2016.10.028.
15. Khan MU, Reddy KR, Snguanwongchai T, et al. Polymer brush synthesis on surface modified carbon nanotubes via in situ emulsion polymerization. *Colloid Polym Sci* 2016; 294: 1599–1610. DOI: 10.1007/s00396-016-3922-7.
16. Reddy KR, Sin BC, Yoo CH, et al. Coating of multiwalled carbon nanotubes with polymer nanospheres through microemulsion polymerization. *J Colloid Interf Sci* 2009; 340: 160–165. DOI: http://dx.doi.org/10.1016/j.jcis.2009.08.044.
17. Choi SH, Kim DH, Raghu AV, et al. Properties of graphene/waterborne polyurethane nanocomposites cast from colloidal dispersion mixtures. *J Macromol Sci B* 2012; 51: 197–207. DOI: 10.1080/00222348.2011.583193.
18. Han SJ, Lee HI, Jeong HM, et al. Graphene modified lipophilically by stearic acid and its composite with low density polyethylene. *J Macromol Sci B* 2014; 53: 1193–1204. DOI: 10.1080/00222348.2013.879804.
19. Hassan M, Reddy KR, Haque E, et al. Hierarchical assembly of graphene/polyaniline nanostructures to synthesize free-standing supercapacitor electrode. *Compos Sci Technol* 2014; 98: 1–8. DOI: 10.1016/j.compscitech.2014.04.007.
20. Hassan M, Reddy KR, Haque E, et al. High-yield aqueous phase exfoliation of graphene for facile nanocomposite synthesis via emulsion polymerization. *J Colloid Interf Sci* 2013; 410: 43–51. DOI: 10.1016/j.jcis.2013.08.006.
21. Lee YR, Kim SC, Lee HI, et al. Graphite oxides as effective fire retardants of epoxy resin. *Macromol Res* 2011; 19: 66–71. DOI: 10.1007/s13233-011-0106-7.
22. Son DR, Raghu AV, Reddy KR, et al. Compatibility of thermally reduced graphene with polyesters. *J Macromol Sci B* 2016; 55: 1099–1110. DOI: 10.1080/00222348.2016.1242529.
23. Biani A, Dorigato A, Bonani W, et al. Mechanical behaviour of cyclic olefin copolymer/exfoliated graphite nanoplatelets nanocomposites foamed through supercritical carbon dioxide. *Exp Polym Lett* 2016; 10: 977–989.
24. Dorigato A, Giusti G, Bondioli F, et al. Electrically conductive epoxy nanocomposites containing carbonaceous fillers and in-situ generated silver nanoparticles. *Exp Polym Lett* 2013; 7: 673–682.
25. Dorigato A and Pegoretti A. Effects of carbonaceous nanofillers on the mechanical and electrical properties of crosslinked poly(cyclooctene). *Polym Eng Sci* 2017; 57: 537–543. DOI: 10.1002/pen.24449.
26. Pedrazzoli D, Dorigato A and Pegoretti A. Monitoring the mechanical behaviour of electrically conductive polymer nanocomposites under ramp and creep conditions. *J Nanosci Nanotechnol* 2012; 12: 4093–4102.

27. Pedrazzoli D, Dorigato A and Pegoretti A. Monitoring the mechanical behaviour under ramp and creep conditions of electrically conductive polymer composites. *Compos A Appl Sci Manuf* 2012; 43: 1285–1292.
28. Maiti A, Svizhenko A and Anantram MP. Electronic transport through carbon nanotubes: effects of structural deformation and tube chirality. *Phys Rev Lett* 2002; 88: 126805.
29. Ou R, Gerhardt RA, Marrett C, et al. Assessment of percolation and homogeneity in ABS/carbon black composites by electrical measurements. *Compos B Eng* 2003; 34: 607–614.
30. Terranova ML, Orlanducci S, Fazi E, et al. Organization of single-walled nanotubes into macro-sized rectangularly shaped ribbons. *Chem Phys Lett* 2003; 381: 86–93.
31. Kumar R. Nano-composite polymer gel electrolytes containing ortho nitro benzoic acid: role of dielectric constant of solvent and fumed silica. *Indian J Phys* 2015; 89: 241–248.
32. Kumar R, Arora N, Sharma S, et al. Electrical characterization of nano-composite polymer gel electrolytes containing NH4BF4 and SiO2: role of donor number of solvent and fumed silica. *Ionics* 2016; 23: 2761–2766.
33. Kumar R and Sekhon SS. Conductivity modification of proton conducting polymer gel electrolytes containing a weak acid (ortho-hydroxy benzoic acid) with the addition of PMMA and fumed silica. *J Appl Electrochem* 2009; 39: 439–445.
34. Sharma S, Dhiman N, Pathak D, et al. Effect of nano-size fumed silica on ionic conductivity of PVdF-HFP-based plasticized nano-composite polymer electrolytes. *Ionics* 2016; 22: 1865–1872.
35. Singh B, Kumar R and Sekhon SS. Conductivity and viscosity behaviour of PMMA based gels and nano dispersed gels: role of dielectric constant of the solvent. *Solid State Ion* 2005; 176: 1577–1583.
36. Fakirov S. *Handbook of thermoplastic polyesters*. Weinheim (Germany): Wiley-VCH, 2002.
37. Dorigato A, Brugnara M, Giacomelli G, et al. Thermal and mechanical behaviour of innovative melt-blown fabrics based on polyamide nanocomposites. *J Ind Text* 2016; 45 1504–1515. DOI: 10.1177/1528083714564633.
38. Chopra S, Deshmukh KA and Peshwe D. Theoretical prediction of interfacial properties of PBT/CNT nanocomposites and its experimental evaluation. *Mech Mater* 2017; 109: 11–17. DOI: 10.1016/j.mechmat.2017.03.012.
39. Gnanasekaran K, Heijmans T, van Bennekom S, et al. 3D printing of CNT- and graphene-based conductive polymer nanocomposites by fused deposition modeling. *Appl Mater Today* 2017; 9: 21–28. DOI: 10.1016/j.apmt.2017.04.003.
40. Kim JY. The effect of carbon nanotube on the physical properties of poly(butylene terephthalate) nanocomposite by simple melt blending. *J Appl Polym Sci* 2009; 112: 2589–2600. DOI: 10.1002/app.29560.
41. Piesowicz E, Irska I, Bratychak M, et al. Poly(butylene terephthalate)/carbon nanotubes nanocomposites. Part I. Carbon nanotubes functionalization and in situ synthesis. *Polimery/Polymers* 2015; 60: 680–685.
42. Piesowicz E, Irska I, Bryll K, et al. Poly(butylene terephthalate/carbon nanotubes nanocomposites. Part II. Structure and properties. *Polimery/Polymers* 2016; 61: 24–30.
43. Saligheh O, Forouharshad M, Arasteh R, et al. The effect of multi-walled carbon nanotubes on morphology, crystallinity and mechanical properties of PBT/MWCNT composite nanofibers. *J Polym Res* 2013; 20: 65. DOI: 10.1007/s10965-012-0065-5.
44. Wu F and Yang G. Synthesis and properties of poly(butylene terephthalate)/multiwalled carbon nanotube nanocomposites prepared by in situ polymerization and in situ compatibilization. *J Appl Polym Science* 2010; 118: 2929–2938. DOI: 10.1002/app.32625.

45. Yang W, Zhou H, Yang B, et al. Facile preparation of modified carbon nanotube-reinforced PBT nanocomposites with enhanced thermal, flame retardancy, and mechanical properties. *Polym Compos* 2016; 37: 1812–1820. DOI: 10.1002/pc.23354.
46. Yin H, Dittrich B, Farooq M, et al. Carbon-based nanofillers/poly(butylene terephthalate): thermal, dielectric, electrical and rheological properties. *J Polym Res* 2015; 22: 140. DOI: 10.1007/s10965-015-0785-4.
47. Dorigato A, Brugnara M and Pegoretti A. Synergistic effects of carbon black and carbon nanotubes on the electrical resistivity of poly(butylene-terephthalate) nanocomposites. *Adv Polym Technol* (in press)
48. Paiva MC, Simon F, Novais RM, et al. Controlled functionalization of carbon nanotubes by a solvent-free multicomponent approach. *ACS Nano* 2014; 4: 7379–7386. DOI: 10.1021/nn1022523.
49. Novais RM, Simon F, Pötschke P, et al. Poly(lactic acid) composites with poly(lactic acid)--modified carbon nanotubes. *J Polym Sci A Polym Chem* 2013; 51: 3740–3750. DOI: 10.1002/pola.26778.
50. Machado AV, Covas JA and Van Duin M. Evolution of morphology and of chemical conversion along the screw in a corotating twin-screw extruder. *J Appl Polym Sci* 1999; 71: 135–141. DOI: 10.1002/(SICI)1097-4628(19990103)71:1<135::AID-APP16>3.0.CO;2-M.
51. Illers KH. Heat of fusion and specific volume of poly(etylene terephthalate) and poly(butylene terephthalate). *Colloids Polym Sci* 1980; 258: 117–124.
52. Martins JA, Cruz VS and Paiva MC. Flow activation volume in composites of polystyrene and multiwall carbon nanotubes with and without functionalization. *Macromolecules* 2011; 44: 9804–9813.
53. Cassagnau P. Melt rheology of organoclay and fumed silica nanocomposites. *Polymer* 2008; 49: 2183–2196. DOI: 10.1016/j.polymer.2007.12.035.
54. Dorigato A, Pegoretti A and Frache A. Thermal stability of high density polyethylene–fumed silica nanocomposites. *J Therm Anal Calorim* 2012; 109: 863–873.
55. Garcia N, Hoyos M, Guzman J, et al. Comparing the effect of nanofillers as thermal stabilizers in low density polyethylene. *Polym Degrad Stab* 2009; 94: 39–48.
56. Leszczynska A, Njuguma J, Pielichowski K, et al. Polymer/montmorillonite nanocomposites with improved thermal properties: Part I. Factors influencing thermal stability and mechanisms of thermal stability improvement. *Thermochimica Acta* 2007; 453: 75–96.
57. Lazzeri A, Zebarjad SM, Pracella M, et al. Filler toughening of plastics. Part 1—the effect of surface interactions on physico-mechanical properties and rheological behaviour of ultrafine CaCO3/HDPE nanocomposites. *Polymer* 2005; 46: 827–844.
58. Costa P, Silva J, Ansón-Casaos A, et al. Effect of carbon nanotube type and functionalization on the electrical, thermal, mechanical and electromechanical properties of carbon nanotube/styrene–butadiene–styrene composites for large strain sensor applications. *Compos B Eng* 2014; 61: 136–146. DOI: 10.1016/j.compositesb.2014.01.048.